

## Developing an energy rating for bifacial photovoltaic modules

Vogt, Malte Ruben; Pilis, Giorgos; Zeman, Miro; Santbergen, Rudi; Isabella, Olindo

**DOI**

[10.1002/pip.3678](https://doi.org/10.1002/pip.3678)

**Publication date**

2023

**Document Version**

Final published version

**Published in**

Progress in Photovoltaics: research and applications

**Citation (APA)**

Vogt, M. R., Pilis, G., Zeman, M., Santbergen, R., & Isabella, O. (2023). Developing an energy rating for bifacial photovoltaic modules. *Progress in Photovoltaics: research and applications*, 31(12), 1466-1477. <https://doi.org/10.1002/pip.3678>

**Important note**

To cite this publication, please use the final published version (if applicable).  
Please check the document version above.


**Copyright**

Other than for strictly personal use, it is not permitted to download, forward or distribute the text or part of it, without the consent of the author(s) and/or copyright holder(s), unless the work is under an open content license such as Creative Commons.

**Takedown policy**

Please contact us and provide details if you believe this document breaches copyrights.  
We will remove access to the work immediately and investigate your claim.

# Developing an energy rating for bifacial photovoltaic modules

Malte Ruben Vogt  | Giorgos Pilis | Miro Zeman | Rudi Santbergen |  
Olindo Isabella

Delft University of Technology, PVMD,  
Mekelweg 4, Delft, 2628CD, The Netherlands

## Correspondence

Malte Ruben Vogt, Delft University of  
Technology, PVMD, Mekelweg 4, 2628CD  
Delft, The Netherlands.  
Email: [m.r.vogt@tudelft.nl](mailto:m.r.vogt@tudelft.nl)

## Abstract

The photovoltaic (PV) module energy rating standard series IEC 61853 does not cover bifacial PV modules. However, the market share of bifacial PV modules has dramatically increased in recent years and is projected to grow. This work demonstrates how Parts 3 and 4 of the IEC 61853 standard could be extended to bifacial modules. First, we develop an irradiance model that uses the data already given in the standard IEC 61853-4 to calculate the irradiance on the rear side of the module. Second, we propose a way to extend the energy yield calculation algorithm IEC 61853-3 to include bifacial modules and make it available to the PV community. This rear irradiance and bifacial energy yield calculation procedure is tested using real outdoor measurements for a nine-month period with a root mean square difference between measured and simulated energy yield of 4.65%. To conclude, we investigate the impact of different climates and normalization on the bifacial module energy rating results.

## KEYWORDS

bifacial PV module, energy rating, energy yield, IEC61853, PV module, PV module performance, view factor

## 1 | INTRODUCTION

Photovoltaic (PV) modules are typically evaluated operating under standard test conditions (STCs)<sup>1</sup> with a fixed operating temperature of 25°C and front side irradiance of 1000 W/m<sup>2</sup> with normal incidence and AM1.5G reference spectrum.<sup>2</sup> However, in practice outdoors in nearly all climates, PV modules will never operate at those conditions. Energy ratings are a measure to evaluate PV modules over 1 year full of operating conditions in different climates instead of just one. Consequently, PV module energy ratings include evaluation of module performance under irradiance from various directions, with various spectra and intensities as well as different operating temperatures over one full year.

The scientific community has proposed and discussed many different approaches to calculate energy ratings.<sup>3–14</sup> It is important to

distinguish between energy yield prediction and energy rating as they are often confused. The goal of an energy yield prediction is to forecast the energy yield of a given system at a specific location as accurately as possible. Thus, it requires several years of location specific meteorological data. In contrast, the goal of an energy rating is to compare the performance of PV modules in a given climate, thus comparability and reproducibility become a priority therefore typically one-year long reference climates are used instead of site-specific meteorological data.

The IEC 61853 series<sup>15–18</sup> defines a standard method to calculate PV module energy ratings. Recently, an intercomparison of more than 10 different research organizations demonstrated that they could calculate the energy rating of two modules with less than 0.1% deviation across all climates,<sup>19</sup> highlighting the comparability of IEC 61853. The standard series was completed in 2018 and consists of four parts. Part

This is an open access article under the terms of the [Creative Commons Attribution](https://creativecommons.org/licenses/by/4.0/) License, which permits use, distribution and reproduction in any medium, provided the original work is properly cited.

© 2023 The Authors. Progress in Photovoltaics: Research and Applications published by John Wiley & Sons Ltd.

1<sup>15</sup> deals with the measurement of the so-called power matrix, which consists of module power values for a range of irradiance  $G$  and module temperature values  $T_{\text{mod}}$ , whereas Part 2<sup>16</sup> defines methods to measure the module's operating temperature, spectral response, and dependency on the incidence angle. The reference climates with hourly irradiation, temperature, wind speed, and angle of incidence data are defined in Part 4.<sup>18</sup> Part 3<sup>17</sup> is at the heart of the standard series tying the measured module and the climate data together in an energy yield and rating calculation algorithm. IEC 61853-3 states that it applies to monofacial PV modules<sup>17</sup> explicitly excluding bifacial PV modules.

Bifacial modules can convert irradiance from the front and rear side, enabling higher energy yields without more complicated fabrication procedures.<sup>20–31</sup> Consequently, the market share of bifacial modules has dramatically increased from 2% in 2016<sup>32</sup> to 28% in 2021<sup>33</sup> and is projected to grow to about 60% by 2032,<sup>33</sup> indicating the need to update the standard to bifacial modules.

A technical report<sup>34</sup> has taken a first step in the development of an energy rating for bifacial modules; however, it is mainly focused on Parts 1 and 2. For Parts 3 and 4, it gives no equations for deriving the rear irradiance or how to deal with the rear irradiance in the energy rating calculation. In this paper, we introduce an alternative detailed approach on how Parts 3 and 4 of the IEC 61853 standard could be extended to bifacial modules to further the scientific discussion.

The main additions of this work are (1) a detailed description of the calculation procedure for rear irradiance including a comprehensive set equations for rear irradiance and bifacial module energy rating calculation. (2) The ground reflected rear irradiance is introduced as a separate climate parameter, which is treated properly in the angular correction step. (3) Our approach is applied to all six climates, and the monthly irradiation distribution is discussed, and the resulting data are downloadable. (4) An initial test of our calculation procedure is conducted by comparison with outdoor measurement data rather than just by calculating energy ratings. (5) Two bifacial energy rating definitions are discussed and compared. (6) The impact of different bifaciality values on the bifacial energy ratings is analyzed. (7) We analyze the differences in the impact of the applied irradiation corrections for both sides of the module.

Our work is organized as follows: In Section 2, we show how the climate data from Part 4 could be expanded to have all the irradiance values to consider bifacial modules. The irradiance results are also provided as Supporting information (Data S1–S6) to this work. Section 3 deals with adjusting energy yield calculation algorithm from Part 3 of IEC 61863 to bifacial modules. It also contains a test of the bifacial module energy yield calculation procedure. The energy rating for bifacial modules is defined and discussed in Section 4, before we conclude in Section 5.

## 2 | REAR IRRADIANCE CALCULATION AND RESULTS

In this section, we introduce the model to calculate the rear irradiance and discuss the results. Note that the rear irradiance calculation would

only have to be performed when creating the bifacial module energy rating climate data and not by every user. It extends the climate data from IEC 61853-4 to provide additional rear irradiance components necessary for bifacial modules. To further scientific discussions, we publish Supporting information (Data S1–S6) to this paper containing the hour results of Equations (1)–(5) for each climate for a fixed albedo of 0.2.

### 2.1 | Rear irradiance calculation procedure

To calculate the energy rating of a bifacial PV module, the irradiance incidence on both faces of the module must be available for calculation; however, the current standard contains only front side irradiance. Thus, we develop an irradiance model that uses the data already given in the standard IEC 61853-4<sup>18</sup> to calculate the irradiance on the rear side of the module  $G_r$  according to

$$G_r = B_r + D_r + D_g. \quad (1)$$

We split the rear irradiance ( $G_r$ ) into three components: beam direct ( $B_r$ ), sky diffuse ( $D_r$ ), and ground reflected diffuse ( $D_g$ ) irradiance, all in-plane of the rear side of the module, given by Equations (3)–(5).

The hourly incidence angle on the rear side of the module  $\theta_r$  is calculated as

$$\theta_r = \cos^{-1} \left( \cos(90^\circ - \alpha_s) * \cos(180^\circ - \beta) + \sin(90^\circ - \alpha_s) * \sin(180^\circ - \beta) * \cos(A_s - A_{mr}) \right) \quad (2)$$

where  $\alpha_s$  is the hourly solar elevation given in the standard,  $\beta$  is the module tilt angle,  $A_s$  is the sun azimuth angle, and  $A_{mr}$  is the azimuth angle of the module rear side, which is defined as facing away from the equator in the standard. Equation (2) only applies for rear incidence angles smaller than  $90^\circ$ , as the standard does for the front side, we set all other angles to  $90^\circ$ . Note that we use  $20^\circ$  module tilt angle in order to enable a comparison of monofacial and bifacial module energy ratings, as the monofacial standard fixes the angle to  $20^\circ$  for all climates irrespective of what the optimum tilt for the climate might be. Different mounting options such as east–west vertical or tracking would enhance the exploitation of the bifacial aspect but would make comparison with the current monofacial standard challenging, which is a core focus of this work. The hourly values for the sun azimuth angle  $A_s$  and the direct normal irradiance (DNI) are calculated as described in Appendix A.1 as they are not published in IEC 61853-4.<sup>18</sup> The direct in-plane rear irradiance  $B_r$  is calculated via the following equation:

$$B_r = \text{DNI} * \cos(\theta_r). \quad (3)$$

The direct in-plane rear irradiance only applies when the sun is located behind the module resulting in a rear incidence angle  $\theta_r < 90^\circ$ .

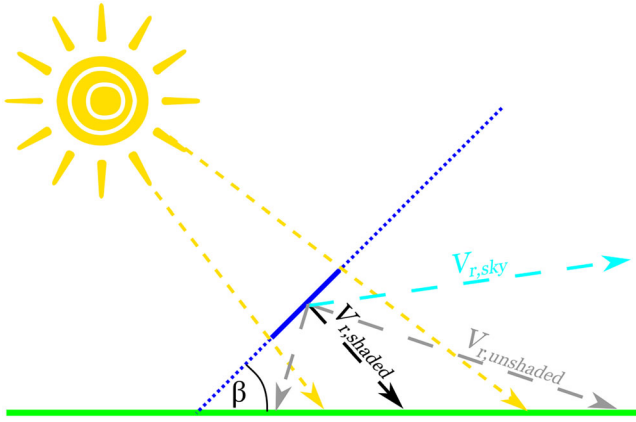


**FIGURE 1** View factors from the rear side of the module to the sky and to shaded and not shaded grounds. [Colour figure can be viewed at [wileyonlinelibrary.com](https://onlinelibrary.wiley.com/doi/10.1002/pep.3678)]

We select a view factor approach to model the rear irradiance as it is fast enough to calculate six full years of hourly irradiance scenarios. Note that this approach assumes uniform irradiance on to the module plane. Considering nonuniformity would most certainly require knowledge of the position of each cell and their operating points to calculate the impact on the module power correctly, which would greatly increase the complexity of calculating an energy rating. Several studies suggest<sup>35–37</sup> that the impact of nonuniformity is small for low albedo and tilt angle combinations such as 0.2 and 20°. The 2D view factor model assumes one infinite row of PV modules with a certain module length and tilt.

Figure 1 shows how the view from the rear side of the module can be divided into three view factors for the purpose of calculating the indirect irradiance on the rear side of the module:

- The view to the sky ( $V_{r,sky}$ ), which receives the sky diffuse rear irradiance ( $D_r$ ).
- The view to the unshaded ground ( $V_{r,unshaded}$ ), where the ground receives the global horizontal irradiance (GHI).
- The view to the shaded ground ( $V_{r,shaded}$ ), where the ground receives the diffuse horizontal irradiance (DHI).

Using more view factors with a finer resolution as in Marion et al.<sup>38</sup> would most likely be advantageous in more detailed soundings or if a different angular correction method would be applied in the energy rating calculation.

The diffuse in-plane rear irradiance  $D_r$  is calculated using the Perez model.<sup>39,40</sup> As such

$$D_r = DHI \left[ (1 + F_1) \frac{1 + \cos(180^\circ - \beta)}{2} + F_1 \left( \frac{\alpha}{b} \right) + F_2 \sin(180^\circ - \beta) \right], \quad (4)$$

where  $\alpha = \max[0, \cos(\theta_r)]$ ;  $b = \max[\cos(85^\circ), \cos(90^\circ - \alpha_s)]$ ; and  $F_1$  and  $F_2$  are the circumsolar and horizon brightness coefficients, respectively, all as given by Perez et al.<sup>39,40</sup>

Our 2D view factor model that considers shading of the ground by the PV module is used to calculate ground reflected irradiance  $D_g$ ,

$$D_g = \alpha_g (DHI * V_{r,shaded} + GHI * V_{r,unshaded}), \quad (5)$$

where  $\alpha_g$  is the ground albedo, and the view factor equations can be found in Appendix A.2. The view factors depend on the exact module mounting conditions. The view factors are derived based on our extension of the work by Appelbaum.<sup>41</sup>

The hourly rear side in-plane irradiance  $G_r$  is then given by the sum of all three parts (Equation 1). As only the front side global in-plane irradiance is given in spectrally ( $R(\lambda)$ ) resolved form in the standard, we also only consider the rear side global in-plane irradiance spectral resolved  $R_r(\lambda)$  via

$$R_r(\lambda) = G_r * \frac{R(\lambda)}{G_f}, \quad (6)$$

where  $G_f$  is the global front side in-plane irradiance given in the standard, thus giving the module rear side irradiance the same spectral distribution as the front side. This choice is made because the direct and diffuse spectra are not published in Part 4, which prevents us from making Equations (3)–(5) fully spectrally resolved. Note that the algorithm in the following section would also work, if the spectra on front and rear side would be different. So, if more information would be made available, it could still be used to calculate bifacial energy ratings.

## 2.2 | Irradiance results for the reference climates

We run rear irradiance model for each climate and hour of the year with an albedo of 0.2, a module mounting height of 1 m defined from the lower edge of the module, a module length of 2 m, and a module tilt angle of 20° to keep consistency with the monofacial standard. Figure 2a shows the rear irradiation distribution for the temperate coastal climate. The ground reflected light accounts for 88% of the rear irradiation, whereas the direct light accounts for less than 1%. A monthly irradiation comparison (Figure 2b) reveals that the differences are largest in the summer months. The rear irradiation distribution for the five climates not shown here is in Appendix A.3 as Figures A1–A5.

The sum of the yearly in-plane front  $H_f$  and rear irradiation  $H_r$  is listed in Table 1 for all climates from IEC 61853-4. In the brackets, we give the bifacial irradiation gain calculated as follows  $H_r/H_f$ . The tropical humid climate receives the highest bifacial irradiation gain of 19.4%, whereas subtropical arid climate receives the lowest gain of 15.7%. The climates with the most diffuse light (temperate coastal and tropical humid) have the highest bifacial irradiation gains and vice versa. Note that these exact values are strongly dependent on albedo, mounting height, module length, module tilt and our assumptions of a single infinite row and uniform irradiance. The hourly irradiance values are available in Data S1–S6 as separate files.

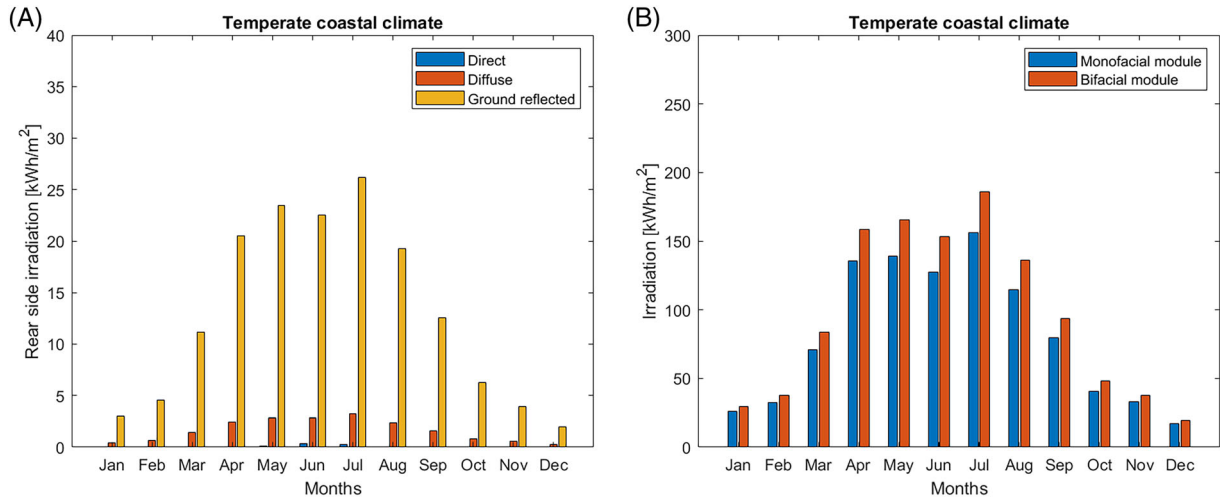


**FIGURE 2** Results of our rear irradiance model. (a) Distribution of light on the rear of the PV module. (b) Comparison of monthly irradiation for mono- and bifacial modules in the temperate coastal climate. [Colour figure can be viewed at [wileyonlinelibrary.com](https://onlinelibrary.wiley.com/doi/10.1002/ep.3678)]

**TABLE 1** Yearly in-plane irradiation on bifacial modules and bifacial irradiation gain compared with monofacial modules.

Climate	Bifacial irradiation [kWh/m <sup>2</sup> ] (bifacial gain)
Temperate coastal	1148.7 (+18.1%)
Temperate continental	1472.2 (+16.3%)
Subtropical coastal	1755.3 (+17.3%)
Tropical humid	2003.1 (+19.4%)
High elevation	2482.6 (+16.1%)
Subtropical arid	2656.2 (+15.7%)

for the rear irradiation. The equations for rear beam irradiance use the rear incidence angle  $\theta_r$  and as the equations for rear sky diffuse irradiance both use the angular loss coefficient of the rear side  $a_{r,r}$ . Because the rear is dominated by ground reflected irradiance (see Figure 2), we also include the correction for ground reflected irradiance. The corrected ground reflected irradiance  $D_{g,corr,j}$  is given by

$$D_{g,corr,j} = D_{g,j} \left\{ 1 - \exp \left[ -\frac{1}{a_{r,r}} \left( \frac{4}{3\pi} \left( \sin \gamma + \frac{\gamma - \sin \gamma}{1 + \cos \gamma} \right) + \left( \frac{a_{r,r}}{2} - 0.154 \right) \left( \sin \gamma + \frac{\gamma - \sin \gamma}{1 + \cos \gamma} \right)^2 \right) \right] \right\}, \quad (7)$$

### 3 | BIFACIAL ENERGY YIELD CALCULATION ALGORITHM AND TEST

Now that we have the necessary rear irradiance data, we adjust the energy yield calculation algorithm of the standard from monofacial to bifacial modules. Then we test the extended algorithm using data from outdoor measurements of a bifacial PV system.<sup>31</sup>

#### 3.1 | Calculation flow

In this subsection, we show how the energy yield calculation algorithm defined in IEC 61853 Part 3<sup>17</sup> can be extended to bifacial modules. Figure 3 shows the proposed algorithm for the calculation of the bifacial module energy yield and rating. To be consistent and thus comparable with monofacial IEC 61853-3 standard, we keep the four main calculation steps. We follow the best practice guidelines<sup>19</sup> established for the front side, except where the bifacial nature of the module requires us to make the adjustments discussed in the following.

The first step is the correction for angular losses; like the standard, we use the model of Martin and Ruiz<sup>42,43</sup> for this purpose. In contrast to the standard, we apply it twice once for the front and once

where  $a_{r,r}$  is the angular loss coefficient of the rear side of the bifacial PV module and  $\gamma = 180^\circ - \beta$ . The corrected beam  $B_{r,corr,j}$  and diffuse irradiance  $D_{r,corr,j}$  are calculated via the same equations as the front side with rear side versions of in-plane beam irradiance  $B_{r,j}$ , angle of incidence  $\theta_{r,j}$ , angular loss coefficient  $a_{r,r}$ , in-plane diffuse irradiance  $D_{r,j}$ , tilt  $\gamma$  replacing their front side counterparts from the standard, and index  $j$  runs through all hours of the year. The three angular corrected rear side irradiance components are summed up to calculate the angular corrected rear side in-plane irradiance  $G_{r,corr,AOI,j} = B_{r,corr,j} + D_{r,corr,j} + D_{g,corr,j}$ .

The second step is the spectral correction, which we do separately for the front and rear side. The spectral correction follows the best practice guidelines<sup>19</sup> established for the front side. Replacing the front side input variables with their rear side counterparts, we derive the equation

$$G_{r,corr,j} = 1000 \cdot \frac{\int_{\lambda_s}^{\lambda_e} S_r(\lambda) \cdot R_{r,corr,AOI,j}(\lambda) \cdot d\lambda}{\int_{\lambda_s}^{\lambda_e} S_r(\lambda) \cdot R_{STC}(\lambda) \cdot d\lambda}, \quad (8)$$

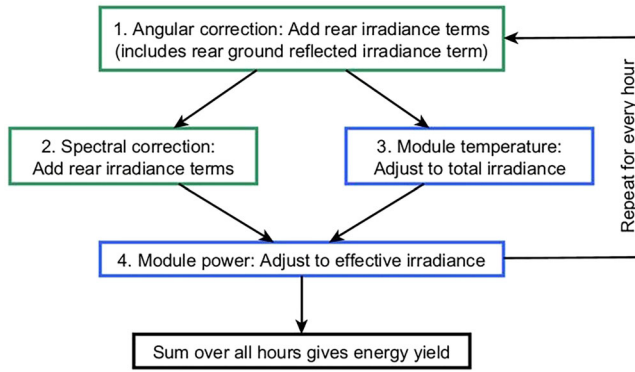


**FIGURE 3** Proposed calculation procedure for energy ratings of bifacial modules. The same four main steps as the monofacial IEC 61853-3 standard. The first major change is that the irradiance corrections steps (green) are applied twice once for the front and once for the rear side. The second is that the module temperature and power calculation steps (blue) now use the total or effective irradiance. [Colour figure can be viewed at [wileyonlinelibrary.com](https://onlinelibrary.wiley.com)]

where  $G_{r,corr,j}$  is the hourly spectral corrected rear side irradiance;  $\lambda_s$  and  $\lambda_e$  are the start and end wavelength of 306.8 nm and 3991 nm, respectively;  $S_r(\lambda)$  is the spectral response of the PV module rear side;  $R_{STC}(\lambda)$  is the AM1.5G reference spectrum<sup>2</sup>; and  $R_{r,corr,AOI,j}(\lambda)$  is the multiplication of spectrally resolved in-plane irradiance  $R_{r,j}(\lambda)$  (from Equation 6) with the ratio of angular corrected  $G_{r,corr,AOI,j}$  and uncorrected  $G_{r,j}$  rear side in-plane irradiance.

Before the module operating temperature is calculated, we sum up the angular corrected front ( $G_{f,corr,AOI,j}$ ) and rear side ( $G_{r,corr,AOI,j}$ ) irradiances to calculate the total angular corrected irradiance

$$G_{tot,corr,AOI,j} = G_{f,corr,AOI,j} + G_{r,corr,AOI,j}. \quad (9)$$

As in the standard, the Faïman model<sup>44</sup> is used to calculate the module operating temperature ( $T_{mod,j}$ )

$$T_{mod,j} = T_{amb,j} + \frac{G_{tot,corr,AOI,j}}{u_0 + u_1 v_j}, \quad (10)$$

where  $T_{amb,j}$  is the ambient temperature,  $v_j$  the wind speed, and  $u_0$  and  $u_1$  are the thermal coefficients of the PV module. Note that the Faïman model has not been updated for the use of bifacial modules. Thus, we adjusted the Faïman model<sup>44</sup> and substituted the front irradiance for the total irradiance. This contains the assumption that the rear side absorption for bifacial modules is much higher for bifacial modules than for monofacial ones, which typically have a white backsheet. Further studies on how to adjust the Faïman temperature model to bifacial modules are strongly recommended, but are too extensive for this work, which focuses on PV module energy ratings.

Prior to calculating the module power output, the effective spectrally corrected irradiance ( $G_{eff,corr,j}$ ) needs to be determined according to

$$G_{eff,corr,j} = G_{f,corr,j} + b_f * G_{r,corr,j}, \quad (11)$$

where  $b_f$  is the bifaciality factor of the PV module power. The bifaciality factor is the ratio between the rear side module power, when this side is illuminated under STC whereas the front side is covered, and the front side module power output when the module is flipped. Note that the bifaciality is not used in Equation (9), because the irradiance, which the rear side of the module could not convert into electrical power, will in most cases still increase the module temperature.

The module power  $P_{mod,j}$  is calculated interpolating the so-called module power matrix to the hourly operating temperatures and irradiances. The only change from the best practice guidelines<sup>19</sup> is that we interpolate or extrapolate to the effective spectrally corrected irradiance ( $G_{eff,corr,j}$ ) from Equation (11) instead of just the front side component. We see the adaptation from front side to effective irradiance as similar to the equivalent irradiance method for determining power output of a bifacial module under bifacial standard test conditions (BSTCs)<sup>45</sup>, while illuminating only the front side. Finally, the yearly energy yield  $E_{tot,year}$  is calculated by summing up the module power  $P_{mod,j}$  over all hours of the year according to

$$E_{tot,year} = \sum_{j=1}^{8760} P_{mod,j} * 1 \text{ h}. \quad (12)$$

Note that we add only relatively simple calculation steps (Equations 7–11) and no new type of PV module parameter. Instead, we add rear side versions of the angular loss coefficient ( $a_{r,r}$ ) and the modules spectral response ( $S_r(\lambda)$ ), because the front side counterparts are already in the current IEC 61853 standard, measuring them for the rear side and the front side only slightly increases the effort. Thus, our bifacial energy yield calculation naturally extends PV module energy ratings algorithm from IEC 61853-3 to bifacial modules.

### 3.2 | Test with energy yield measurement data

We use the bifacial ground based reference system next to the floating system introduced by Ziar et al.<sup>31</sup> to check whether the combination of our rear irradiance model (Section 2) and bifacial energy yield calculation algorithm (Section 3.1) can determine the module power output of a bifacial module. For a nine-month period, the module output power, the ambient temperature, the wind speed, and the GHI were measured at the test site. Our calculation procedure also requires the solar altitude and azimuth as well as DHI and DNI. Therefore, we use the PV\_LIB toolbox<sup>46</sup> in Matlab to calculate the sun position and the model by Reindl et al.<sup>47</sup> to decompose GHI into DHI and DNI. We adjust the albedo, module tilt, and module parameters to the ones of the reference system.

Figure 4 shows the comparison between measured (blue) and simulated (orange) energy yield. Over the whole period, the root mean square difference is 4.65% based on comparing hourly values of the measured and simulated energy yield of the bifacial module. Note that



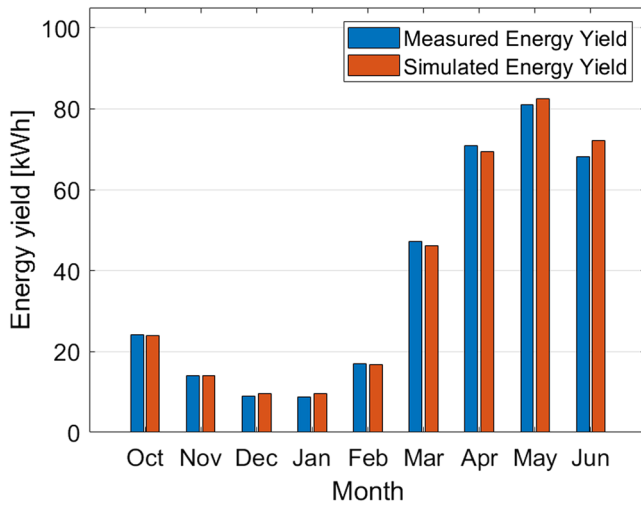


**FIGURE 4** Measured bifacial energy yield at the outdoor test site (blue) and simulated energy yield by the model introduced in this work (orange). Over a nine-month period, the root mean square difference between measured and simulated energy yield is 4.65%. [Colour figure can be viewed at [wileyonlinelibrary.com](http://wileyonlinelibrary.com)]

because only the GHI is measured, we calculated decomposition into direct and diffuse as well as in-plane irradiance, which most likely creates additional deviations as compared to the standard where decomposed in-plane irradiance is given. Nevertheless, the agreement indicates that our algorithm is accurate enough to calculate the bifacial module energy yield for the purpose of creating an energy rating.

## 4 | BIFACIAL ENERGY RATING DEFINITION AND RESULTS

After introducing the bifacial energy yield calculation algorithm and testing it, this section deals with two ways to define the energy rating for bifacial modules and discusses the results in the climates.

### 4.1 | How to define the bifacial energy rating?

The climate specific energy rating (CSER) for monofacial is defined as energy efficiency in the reference climate over 1 year divided by power efficiency under standard test conditions given by the following equation.<sup>17</sup>

$$CSER_{mono} = \frac{E_{f,year}/H_{f,year}}{P_{f,STC}/G_{f,STC}}, \quad (13)$$

where  $E_{f,year}$  is the monofacial energy yield,  $H_{f,year}$  is the yearly in-plane irradiation of the front side,  $P_{f,STC}$  is the module power under STC, and  $G_{f,STC}$  is the STC irradiance. Replacing these measurables by their bifacial module counterparts, we derive

$$CSER_{bif1} = \frac{E_{tot,year}/H_{tot,year}}{P_{BSTC}/G_{BSTC}}, \quad (14)$$

where  $E_{tot,year}$  is the bifacial energy yield,  $H_{tot,year}$  is the yearly in-plane irradiation of the front and rear side,  $P_{BSTC}$  is the module power under BSTC, and  $G_{BSTC}$  is the BSTC irradiance. The disadvantage of this definition is that it is hard to compare bifacial and monofacial modules. This can be best realized, if we try to calculate the  $CSER_{bif1}$  value for monofacial modules or bifacial modules with bifaciality factor of zero. To do this, we insert the following into Equation (14):  $E_{tot,year} = E_{f,year}$ ,  $P_{BSTC} = P_{STC}$ , and  $G_{BSTC} = G_{STC}$ , due to the scaling of BSTC with the bifaciality factor,<sup>29</sup> while  $H_{tot,year} = H_{tot,year}$  remains the same because a monofacial module receives rear side irradiance. Consequently, one would then have  $CSER_{bif1} < CSER_{mono}$  for the same module. The reason behind this is ultimately that the mono- and bifacial energy rating definitions have different yearly in-plane irradiation reference points. Thus, we propose a second definition:

$$CSER_{bif2} = \frac{E_{tot,year}/H_{f,year}}{P_{BSTC}/G_{BSTC}}, \quad (15)$$

which has  $H_{f,year}$  the yearly in-plane irradiation of the front replacing the total irradiation. This solves the comparison problem with the monofacial energy rating in the existing standard by giving  $CSER_{bif2} = CSER_{mono}$ , when repeating the same thought experiment of calculating the bifacial energy rating for monofacial modules.

### 4.2 | Bifacial energy rating in reference climates

To analyze the differences between these definitions, we use the open source data for the monofacial c-Si “module 1” as published by Vogt et al.<sup>19</sup> As no such data are available for bifacial modules, we assume for the purpose of calculating the bifacial energy rating that this module has rear side with the same angular loss coefficient and spectral response as the front side. This completes the PV module input data for our calculation procedure. Note that while we assume the same front and rear side module parameters that due to different values in Part 4, we still perform the separate calculations as described in Section 3. Furthermore, we vary the bifaciality factor with values of 0, 0.5, and 1.

Figure 5 shows the CSER values for bifacial modules according to Approach 1 (circles) and Approach 2 (“x”) for three different bifaciality factors (1 in blue, 0.5 in green, and 0 in red) and the monofacial energy rating (plus). The second approach gives the same CSER value for a bifaciality of zero as the monofacial module, as the modules have identical front sides. In contrast, the first approach always gives a lower CSER even for a bifaciality equal to one. The fact that the first definition is lower for a bifaciality factor of one shows that the rear side energy efficiency is lower than the front side energy efficiency. As desired, both definitions clearly show the advantage

of a higher bifaciality factor. However, due to better comparability with monofacial standard, we recommend the use of the second definition  $CSER_{bif2}$  and focus our further analysis on this definition.

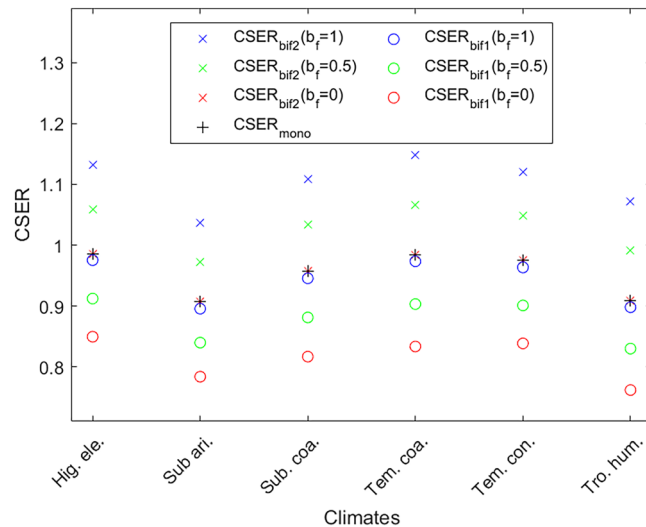


**FIGURE 5** Climate specific energy rating (CSER) for bifacial modules according to Approach 1 (circle) and Approach 2 (“x”) for three different bifaciality factors and the monofacial energy rating (plus). The second approach gives the same CSER value for a bifaciality of zero as the monofacial module, when assuming identical front sides. In contrast, the first approach always gives a lower CSER even for a bifaciality of one. [Colour figure can be viewed at [wileyonlinelibrary.com](https://onlinelibrary.wiley.com)]

Comparing the impact different climates for this second definition bifacial energy rating with the monofacial energy rating, we see the largest difference of 17.9% for bifaciality of one and 9% for bifaciality of 0.5 in the tropical humid climate. While the subtropical arid climate results in the lowest difference in bifacial gains of 14.3% and 7.2% for the bifaciality factors of 1 and 0.5, respectively. The diffuse irradiance fraction in the climates drives this trend.

Additionally, we investigate the impact of the irradiance correction step by skipping them and calculating the bifacial energy rating  $CSER_{bif2}$ . Table 2 lists the results as percentage change in  $CSER_{bif2}$  for same modules as in the previous figure. Having no angle of incidence (AOI) correction increases the energy rating by up to 5.3% for a bifacial module with bifaciality factor of one, but only by up to 2.9% for a module with bifaciality factor of zero. This signifies that the AOI correction of the rear irradiance reduces the PV module energy rating by 2.4%, whereas the front side AOI correction reduces it by 2.9%. Interestingly the rear side irradiation is only 18.1% of the front side irradiation yet they have nearly the same impact on the bifacial energy rating. The fact that angular correction of the front and rear side irradiation has similar impacts holds for all climates.

In fact, in the subtropical arid climate, the climate with the lowest AOI correction impact, both front and rear correction are responsible for a reduction of 1.7%. This implies that having a separate angular rear irradiance correction step is paramount for a bifacial energy rating. Note that the angular by Martin and Ruiz<sup>42,43</sup> was developed for monofacial modules and that these results are based on the assumption that it also can be used to model the rear side of bifacial modules.

**TABLE 2** Effect of irradiance correction on energy bifacial energy rating.

Climate	Bifacial factor	No AOI correction [ $CSER_{bif2}$ change in %]	No spectral correction [ $CSER_{bif2}$ change in %]
Temperate coastal	1	+5.3	−3.2
	0.5	+4.1	−3.0
	0	+2.9	−2.7
Temperate continental	1	+4.5	−2.0
	0.5	+3.5	−1.9
	0	+2.4	−1.7
Subtropical coastal	1	+4.2	−3.1
	0.5	+3.2	−2.8
	0	+2.1	−2.6
Tropical humid	1	+4.2	−2.9
	0.5	+3.2	−2.6
	0	+2.1	−2.4
High elevation	1	+3.8	+1.8
	0.5	+2.9	+1.7
	0	+2.0	+1.6
Subtropical arid	1	+3.4	−0.6
	0.5	+2.5	−0.5
	0	+1.7	−0.5

Abbreviation: AOI, angle of incidence.



Having no spectral correction decreases the energy rating by up to 3.2% for a bifacial module with bifaciality factor of one, but only by up to 2.7% for a module with bifaciality factor of zero. Thus, the rear side is only responsible for a 0.5% change, whereas the front side accounts for 2.7% change in spectral correction. The change is similar or smaller in all other climates. The high elevation climate differs as it is the only climate in which the spectral correction decreases the energy yield and rating; however, the rear side impact is 0.2% compared to 1.6% for the front side. Therefore, rear side has no over proportional impact on the spectral correction. Note that this might change if a drastically different spectral distribution of the rear side is used instead of Equation (6), which inverts the front side distribution to the rear side due to a lack of separate diffuse and direct spectra in IEC 61853-4. Also, having a different PV module with different optical properties for the rear side could change these findings. Therefore, we recommend that this should be investigated further in future work.

## 5 | SUMMARY AND CONCLUSION

In this work, we proposed and evaluated an energy rating for bifacial modules. The missing rear side irradiance data are calculated using a view factor model. The energy yield calculation algorithm uses separate calculation steps for front and rear side angular as well as spectral correction. The rear side angular correction is extended by a term for ground reflected irradiance. The temperature and power calculation steps use the combined total and effective irradiance, respectively. Thus, only relatively simple calculation steps and no measurements, which are not already used for the front side, are added when extending the standard to bifacial modules. This procedure was tested using outdoor measurements over a nine-month period.

We evaluated two different approaches for defining the bifacial CSER and conclude that the second one, using only the front side irradiation for reference, is more advantageous due to better comparability and consistency with the established monofacial standard. Further, we show that the bifacial gain in CSER in a climate is linked to the diffuse fraction of the irradiance. We also provide a first indication that the separate angular correction of rear side irradiance is important for bifacial energy ratings.

## AUTHOR CONTRIBUTIONS

**M. R. Vogt:** Conceptualization; methodology and software; validation; visualization; supervision; writing—original draft; review and editing. **G. Pilis:** Formal analysis; methodology and software; validation; visualization. **M. Zeman:** Supervision; funding acquisition. **R. Santbergen:** Writing—review and editing; supervision; project administration. **O. Isabella:** Writing—review and editing; supervision; funding acquisition.

## ACKNOWLEDGEMENTS

We would like to thank Hesam Ziar for providing the energy yield measurement data for testing.

## DATA AVAILABILITY STATEMENT

The data created by us will be available in the appendix of this article as open source. However, we rely on the data from IEC61853-4, which is under copyright by IEC, so we cannot share any original IEC data.

## ORCID

Malte Ruben Vogt  <https://orcid.org/0000-0003-3924-2456>

## REFERENCES

1. "IEC61836: solar photovoltaic energy systems—terms, definitions and symbols." 2016.
2. "IEC 60904-3: photovoltaic devices—part 3: measurement principles for terrestrial photovoltaic (PV) solar devices with reference spectral irradiance data." 2019.
3. Bonilla Castro J, Schweiger M, Moser D et al. "Climatic rating of photovoltaic modules: different technologies for various operating conditions," IEA-PVPS T13-20:2020, 2021.
4. Vogt MR, Riechelmann S, Gracia-Amillo AM, et al. Interlaboratory comparison of the PV module energy rating standard IEC 61853-3. In: *Presented at the 37th European Photovoltaic Solar Energy Conference and Exhibition, EUPVSEC 2020*:811-816.
5. Huld T, Salis E, Pozza A, Herrmann W, Mülleijans H. Photovoltaic energy rating data sets for Europe. *Sol Energy*. 2016;133:349-362. doi:[10.1016/j.solener.2016.03.071](https://doi.org/10.1016/j.solener.2016.03.071)
6. Huld T, Dunlop E, Beyer HG, Gottschalg R. Data sets for energy rating of photovoltaic modules. *Sol Energy*. 2013;93:267-279. doi:[10.1016/j.solener.2013.04.014](https://doi.org/10.1016/j.solener.2013.04.014)
7. Blakesley JC, Huld T, Mülleijans H, et al. Accuracy, cost and sensitivity analysis of PV energy rating. *Sol Energy*. 2020;203:91-100. doi:[10.1016/j.solener.2020.03.088](https://doi.org/10.1016/j.solener.2020.03.088)
8. Verlinden PJ, Lasich JB. Energy rating of Concentrator PV systems using multi-junction III-V solar cells. In: *2008 33rd IEEE Photovoltaic Specialists Conference, San Diego, CA, USA*. IEEE; May 2008:1-6. doi:[10.1109/PVSC.2008.4922912](https://doi.org/10.1109/PVSC.2008.4922912)
9. Schweiger M, Bonilla J, Herrmann W, Gerber A, Rau U. Performance stability of photovoltaic modules in different climates: electrical stability of PV modules. *Prog Photovolt Res Appl*. 2017;25(12):968-981. doi:[10.1002/pip.2904](https://doi.org/10.1002/pip.2904)
10. Schweiger M. "Performance of PV modules with different technologies and the impact on energy yield in four climatic zones," Dissertation, Technischen Hochschule Aachen, 2017.
11. Dirnberger D, Müller B, Reise C. PV module energy rating: opportunities and limitations: PV module energy rating: opportunities and limitations. *Prog Photovolt: Res Appl*. 2015;23(12):1754-1770. doi:[10.1002/pip.2618](https://doi.org/10.1002/pip.2618)
12. Kenny RP, Friesen G, Chianese D, Bernasconi A, Dunlop ED. Energy rating of PV modules: comparison of methods and approach. In: *Presented at the WCPEC-3, Osaka, Japan*. WCPEC; 2003:2015-2018.
13. Kenny RP, Dunlop ED, Ossensbrink HA, Mülleijans H. A practical method for the energy rating of c-Si photovoltaic modules based on standard tests. *Prog Photovolt: Res Appl*. 2006;14(2):155-166. doi:[10.1002/pip.658](https://doi.org/10.1002/pip.658)
14. Driesse A, Theristis M, Stein JS. A new photovoltaic module efficiency model for energy prediction and rating. *IEEE J Photovoltaics*. 2021;11(2):527-534. doi:[10.1109/JPHOTOV.2020.3045677](https://doi.org/10.1109/JPHOTOV.2020.3045677)
15. "IEC61853-1: PV module performance testing and energy rating—part 1: irradiance and temperature performance measurements and power rating." 2011.
16. "IEC61853-2: PV module performance testing and energy rating—part 2: spectral responsivity, incidence angle and module operating temperature measurements." 2016.

17. "IEC61853-3: PV module performance testing and energy rating—part 3: energy rating of PV modules." 2018.
18. "IEC61853-4: PV module performance testing and energy rating—part 4: standard reference climatic profiles." 2018.
19. Vogt MR, Riechelmann S, Gracia-Amillo AM, et al. PV module energy rating standard IEC 61853-3 intercomparison and best practice guidelines for implementation and validation. *IEEE J Photovoltaics*. 2022;12(3):844-852. doi:[10.1109/JPHOTOV.2021.3135258](https://doi.org/10.1109/JPHOTOV.2021.3135258)
20. Cuevas A, Luque A, Eguren J, del Alamo J. 50 per cent more output power from an albedo-collecting flat panel using bifacial solar cells. *Sol Energy*. 1982;29(5):419-420. doi:[10.1016/0038-092X\(82\)90078-0](https://doi.org/10.1016/0038-092X(82)90078-0)
21. Kopecek R, Libal J. Towards large-scale deployment of bifacial photovoltaics. *Nat Energy*. 2018;3(6):443-446. doi:[10.1038/s41560-018-0178-0](https://doi.org/10.1038/s41560-018-0178-0)
22. Riedel-Lyngskær N, Poulsen PB, Jakobsen ML, Nørgaard P, Vedde J. Value of bifacial photovoltaics used with highly reflective ground materials on single-axis trackers and fixed-tilt systems: a Danish case study. *IET Renew Power Gen*. 2020;14(19):3946-3953. doi:[10.1049/iet-rpg.2020.0580](https://doi.org/10.1049/iet-rpg.2020.0580)
23. McIntosh KR, Abbott MD, Loomis G, et al. Irradiance on the upper and lower modules of a two-high bifacial tracking system. In: *2020 47th IEEE Photovoltaic Specialists Conference (PVSC), Calgary, AB, Canada*. IEEE; Jun. 2020:1916-1923. doi:[10.1109/PVSC45281.2020.9300838](https://doi.org/10.1109/PVSC45281.2020.9300838)
24. Dullweber T, Schulte-Huxel H, Blankemeyer S, et al. Present status and future perspectives of bifacial PERC+ solar cells and modules. *Jpn J Appl Phys*. 2018;57(8S3):08RA01. doi:[10.7567/JJAP.57.08RA01](https://doi.org/10.7567/JJAP.57.08RA01)
25. Nussbaumer H, Janssen G, Berrian D, et al. Accuracy of simulated data for bifacial systems with varying tilt angles and share of diffuse radiation. *Solar Energy*. 2020;197:6-21. doi:[10.1016/j.solener.2019.12.071](https://doi.org/10.1016/j.solener.2019.12.071)
26. Vogt MR, Gewohn T, Bothe K, Schinke C, Brendel R. Impact of using spectrally resolved ground albedo data for performance simulations of bifacial modules. *Energy Procedia*. 2018;22.
27. Blakesley JC, Koutsourakis G, Douglas S, et al. Effective spectral albedo from satellite data for bifacial gain calculations of PV systems. In: *Presented at the 37th European Photovoltaic Solar Energy Conference and Exhibition*; 2020:1292-1297. doi:[10.4229/EUPVSEC20202020-5CO.9.3](https://doi.org/10.4229/EUPVSEC20202020-5CO.9.3)
28. Janssen GJM, Van Aken BB, Carr AJ, Mewe AA. Outdoor performance of bifacial modules by measurements and modelling. *Energy Procedia*. 2015;77:364-373. doi:[10.1016/j.egypro.2015.07.051](https://doi.org/10.1016/j.egypro.2015.07.051)
29. Monokroussos C, Gao Q, Zhang XY, et al. Rear-side spectral irradiance at 1 sun and application to bifacial module power rating. *Prog Photovolt Res Appl*. 2020;28(8):755-766. doi:[10.1002/pip.3268](https://doi.org/10.1002/pip.3268)
30. Sun X, Khan MR, Deline C, Alam MA. Optimization and performance of bifacial solar modules: a global perspective. *Appl Energy*. 2018;212:1601-1610. doi:[10.1016/j.apenergy.2017.12.041](https://doi.org/10.1016/j.apenergy.2017.12.041)
31. Ziar H, Prudon B, Lin FY(V), et al. Innovative floating bifacial photovoltaic solutions for inland water areas. *Prog Photovolt Res Appl*. 2021; 29(7):725-743. doi:[10.1002/pip.3367](https://doi.org/10.1002/pip.3367)
32. VDMA. *International Technology Roadmap for Photovoltaic (ITRPV) 2016 Results*. Eighth Edition; 2017.
33. VDMA. *International Technology Roadmap for Photovoltaic (ITRPV) 2021 Results*. Thirteenth Edition; 2022.
34. Gracia-Amillo AM, Kenny R, Friesen G, Reise C, Lopez-Garcia J. Extension of energy rating to bifacial modules—proposals from the PV-enerate project. *JRC122448*. 2020.
35. Liang TS, Pravettoni M, Singh JP, Wang Y, Khoo YS. Towards IEC TS 60904-1-2: assessing the requirements for irradiance on the non-illuminated side of bifacial PV modules with single light source testing. In: *Presented at the 35th EuPVSEC*; 2018:1017-1023.
36. Lopez-Garcia J, Gali SR, Grau-Luque E, Kenny RP, Sample T. Assessment of the rear irradiance on bifacial silicon PV modules. In: *Presented at the 36th EUPVSEC*; 2019:901-908.
37. Rauer M, Schmid A, Guo F, Neuberger F, Gebhardt P, Hohl-Ebinger J. Comprehensive evaluation of IEC measurement procedures for bifacial solar cells and modules. In: *Presented at the 37th EuPVSEC*; 2020. p. 4CO.2.1.
38. Marion B, MacAlpine S, Deline C, et al. A practical irradiance model for bifacial PV modules. In: *2017 IEEE 44th Photovoltaic Specialist Conference (PVSC), Washington, DC*; Jun. 2017:1537-1542. doi:[10.1109/PVSC.2017.8366263](https://doi.org/10.1109/PVSC.2017.8366263)
39. Perez R, Seals R, Ineichen P, Stewart R, Menicucci D. A new simplified version of the Perez diffuse irradiance model for tilted surfaces. *Sol Energy*. 1987;39(3):221-231. doi:[10.1016/S0038-092X\(87\)80031-2](https://doi.org/10.1016/S0038-092X(87)80031-2)
40. Perez R, Seals R, Michalsky J. All-weather model for sky luminance distribution—preliminary configuration and validation. *Solar Energy*. 1993;50(3):235-245. doi:[10.1016/0038-092X\(93\)90017-1](https://doi.org/10.1016/0038-092X(93)90017-1)
41. Appelbaum J. The role of view factors in solar photovoltaic fields. *Renew Sustain Energy Rev*. 2018;81:161-171. doi:[10.1016/j.rser.2017.07.026](https://doi.org/10.1016/j.rser.2017.07.026)
42. Martin N, Ruiz JM. Calculation of the PV modules angular losses under field conditions by means of an analytical model. *Solar Energy Mater. Sol. Cells*. 2001;70(1):25-38. doi:[10.1016/S0927-0248\(00\)00408-6](https://doi.org/10.1016/S0927-0248(00)00408-6)
43. Martin N, Ruiz JM. Corrigendum to calculation of the PV modules angular losses under field conditions by means of an analytical model. *Solar Energy Mater Sol Cells*. 2012;110:154. doi:[10.1016/j.solmat.2012.11.002](https://doi.org/10.1016/j.solmat.2012.11.002)
44. Faiman D. Assessing the outdoor operating temperature of photovoltaic modules. *Prog Photovolt: Res Appl*. 2008;16(4):307-315. doi:[10.1002/pip.813](https://doi.org/10.1002/pip.813)
45. "IEC TS 60904-1-2 Ed. 1 measurement of current-voltage characteristics of bifacial photovoltaic (PV) devices." 2019.
46. Sandia National Laboratories. "PV\_LIB toolbox." [Online]. [https://pvpmmc.sandia.gov/applications/pv\\_lib-toolbox/](https://pvpmmc.sandia.gov/applications/pv_lib-toolbox/)
47. Reindl DT, Beckman WA, Duffie JA. Evaluation of hourly tilted surface radiation models. *Solar Energy*. 1990;45(1):9-17. doi:[10.1016/0038-092X\(90\)90061-G](https://doi.org/10.1016/0038-092X(90)90061-G)
48. Smets AH, Jäger K, Isabella O, Swaaij RA, Zeman M. *Solar Energy: The Physics and Engineering of Photovoltaic Conversion, Technologies and Systems*. UIT Cambridge Limited; 2016.

## SUPPORTING INFORMATION

Additional supporting information can be found online in the Supporting Information section at the end of this article.

**How to cite this article:** Vogt MR, Pilis G, Zeman M, Santbergen R, Isabella O. Developing an energy rating for bifacial photovoltaic modules. *Prog Photovolt Res Appl*. 2023; 1-12. doi:[10.1002/pip.3678](https://doi.org/10.1002/pip.3678)

## APPENDIX A.

### A.1 | Calculation of DNI and sun azimuth angle

First, we obtain the direct normal irradiance (DNI) from the direct horizontal irradiance ( $B_h$ ) and the solar elevation ( $\alpha_s$ ) given in the standard<sup>18</sup> via

$$DNI = B_h / \cos(\theta_z), \quad (A1)$$

with the sun zenith angle  $\theta_z = 90 - \alpha_s$ .

Next, the sun azimuth angle  $A_s$  is determined using

$$A_s = \text{sign}(\omega) \left| \cos^{-1} \left( \frac{\cos(\theta_z) \sin(\Phi) - \sin(\delta)}{\sin(\theta_z) \cos(\Phi)} \right) \right|, \quad (A2)$$

where  $\omega$  is the hour angle,  $\Phi$  is the latitude of the climate data given in Part 4, and  $\delta$  is the declination angle. To determine the declination angle, we use

$$\begin{aligned} \delta = & (180\pi)(0.006918 - 0.399912 \cos(B) + 0.070257 \sin(B) \\ & - 0.006758 \cos(2B) + 0.000907 \sin(2B) - 0.002697 \cos(3B) \\ & + 0.00148 \sin(3B)), \end{aligned} \quad (A3)$$

where  $B$  is defined by

$$B = (n - 1) \frac{360}{365}, \quad (A4)$$

with  $n$  being the day of the year.

## A.2 | View factors

Figure 1 shows the geometry of our 2D view factor model consisting of a single row of modules with an infinite row length. It is an extension of Appelbaum's work,<sup>41</sup> which considers also the module mounting height above the ground measured from what we would in reality call the front edge of the module but is a point in the 2D. Looking at the projection of the ground to this height, we can see the Appelbaum unshaded ground is equivalent to our unshaded ground behind the module is defined as

$$V_{r,unshaded,2} = \frac{L_m \cos(\beta) + \sqrt{L_m^2 + L_s^2 - 2 * L_m * L_s * \cos(\beta)} - L_s}{2 * L_m}, \quad (A5)$$

where  $L_m$  is the module length,  $\beta$  is the module tilt, and  $L_s$  is the shadow length, which we take from eq. 3.11 by Smets et al.<sup>48</sup> The shaded ground is defined as

$$V_{r,shaded} = \frac{L_m + L_s - \sqrt{L_m^2 + L_s^2 - 2 * L_m * L_s * \cos(\beta)}}{2 * L_m} - V_{r,unshaded,1}, \quad (A6)$$

where the  $V_{r,unshaded,1}$  view factor unshaded ground in front of the module is subtracted from the view factor of Appelbaum's shaded ground. This view factor unshaded ground in front of the module is defined via

$$V_{r,unshaded,1} = \frac{L_m + L_p - \sqrt{L_m^2 + L_p^2 - 2 * L_m * L_p * \cos(\beta)}}{2 * L_m}, \quad (A7)$$

where  $L_p$  is the length of the projection of the unshaded ground in front of the shadow to the module mounting height  $H_g$ . It is calculated via

$$L_p = \frac{L_m * \sin(a)}{\sin(\rho)}, \quad (A8)$$

where  $\rho$  is the missing angle in a triangle of the module tilt and  $\sigma$  is the angle for the unshaded ground in front of the shadow. They are define via

$$\rho = 180 - \sigma - \beta, \quad (A9)$$

$$\sigma = \text{asin} \left( \frac{L_{UG} * \sin(\beta)}{S} \right), \quad (A10)$$

with  $L_{UG}$  being the length of the unshaded ground in from of the module

$$L_{UG} = \frac{H_g}{\tan(\beta)} + \frac{H_g * \cos(A_{mr} - A_s)}{\tan(\alpha_s)} \quad (A11)$$

where  $\alpha_s$  is the hourly solar elevation given in the standard,  $\beta$  is the module tilt angle,  $A_s$  is the sun azimuth angle, and  $A_{mr}$  is the azimuth angle of the module rear side. The side  $S$  is define as

$$S = \sqrt{(L_{UG})^2 + ((E + L_m))^2 - (2 * L_{UG} * (E + L_m) * \cos(\beta))}, \quad (A12)$$

in which  $E$  is the extension of the module towards the ground obtained via

$$E = \frac{H_g}{\sin(\beta)}. \quad (A13)$$

The sum of both unshaded ground view factors

$$V_{r,unshaded} = V_{r,unshaded,1} + V_{r,unshaded,2}, \quad (A14)$$

is used in Equation (5) of this work. Finally, as an initial test we see that

$$V_{r,unshaded} + V_{r,shaded} + V_{r,sky} = 1. \quad (A15)$$

## A.3 | Figures visualizing the monthly irradiance distribution in the other reference climates

We run rear irradiance model for each climate and hour of the year with an albedo of 0.2, a module mounting height of 1 m, a module length of 2 m, and a module tilt angle of 20° to keep consistency with the monofacial standard. In Figures A1–A5, we show the rear irradiation distribution for the five climates not shown in Section 2.2.

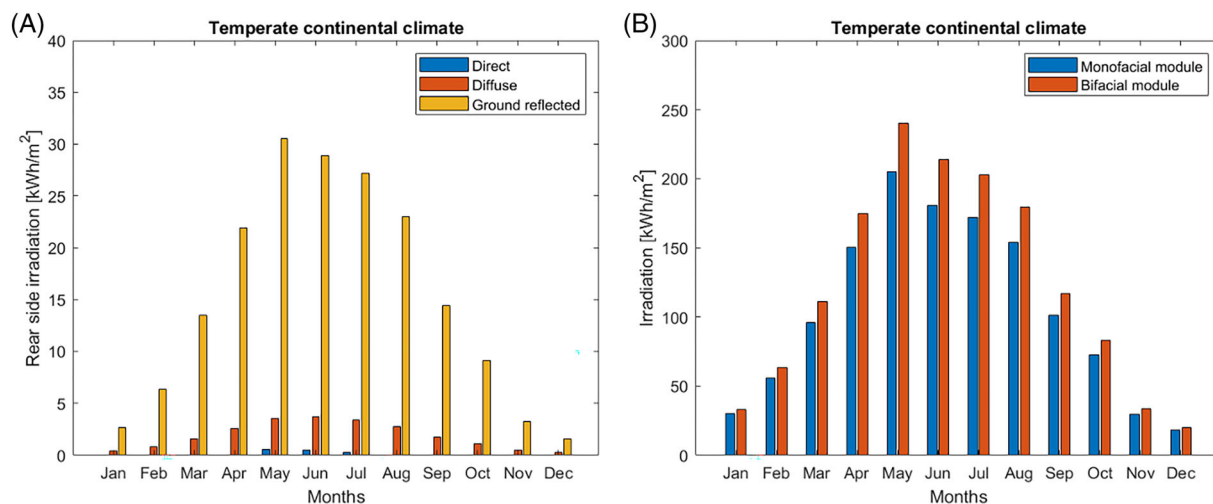


**FIGURE A1** Results of our rear irradiance model applied to the temperate continental climate data. (a) Distribution of light on the rear of the PV module. (b) Comparison of monthly irradiation for mono- and bifacial modules. [Colour figure can be viewed at [wileyonlinelibrary.com](https://onlinelibrary.wiley.com/doi/10.1002/pep.3678)] [wileyonlinelibrary.com](https://onlinelibrary.wiley.com/doi/10.1002/pep.3678)

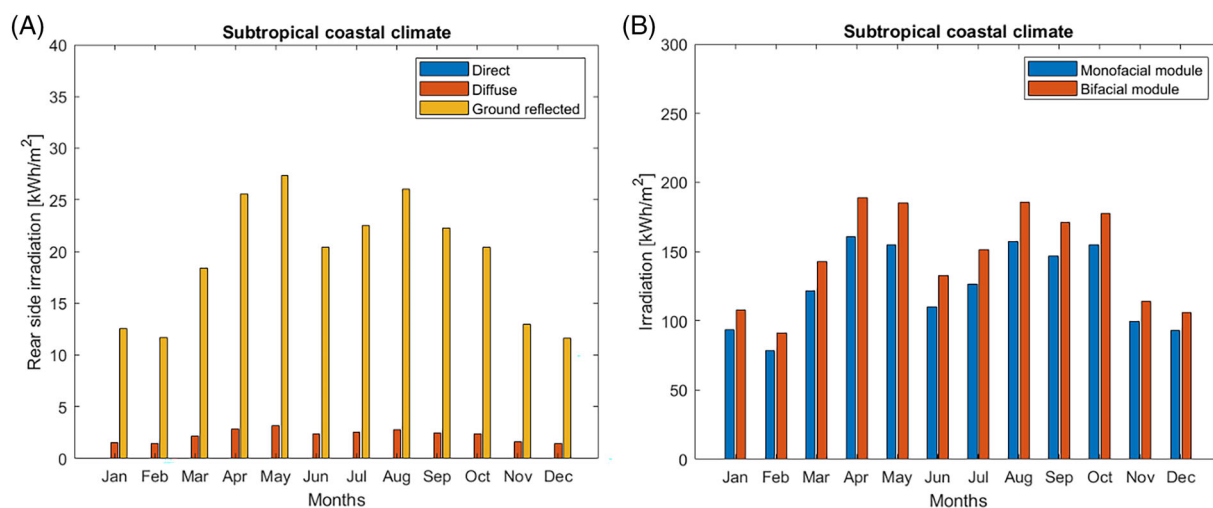


**FIGURE A2** Results of our rear irradiance model applied to the subtropical coastal climate data. (a) Distribution of light on the rear of the PV module. (b) Comparison of monthly irradiation for mono- and bifacial modules. [Colour figure can be viewed at [wileyonlinelibrary.com](https://onlinelibrary.wiley.com/doi/10.1002/pep.3678)] [wileyonlinelibrary.com](https://onlinelibrary.wiley.com/doi/10.1002/pep.3678)

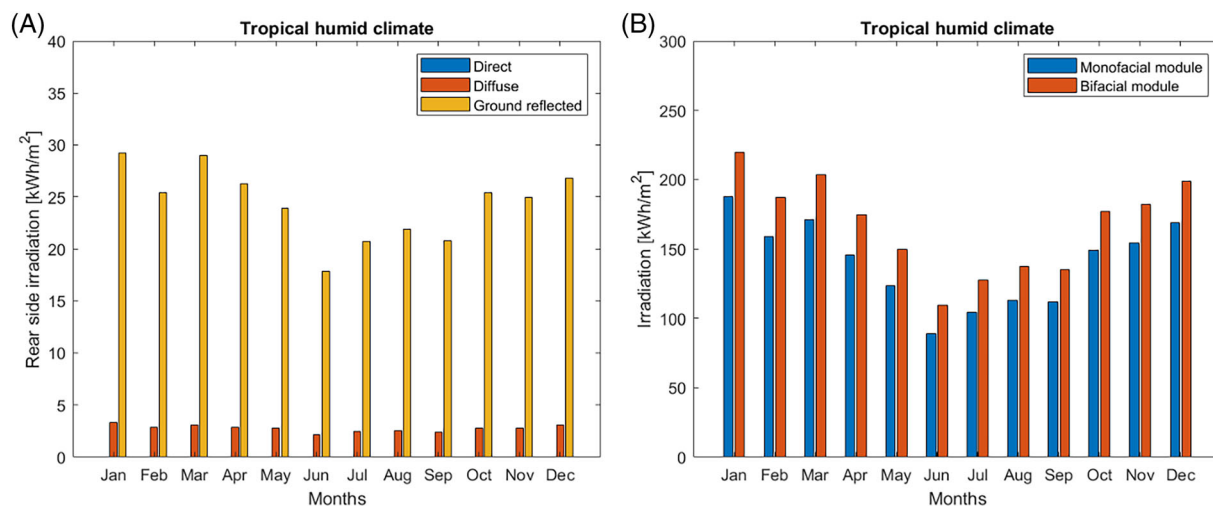


**FIGURE A3** Results of our rear irradiance model applied to the tropical humid climate data. (a) Distribution of light on the rear of the PV module. (b) Comparison of monthly irradiation for mono- and bifacial modules. [Colour figure can be viewed at [wileyonlinelibrary.com](https://onlinelibrary.wiley.com/doi/10.1002/pep.3678)] [wileyonlinelibrary.com](https://onlinelibrary.wiley.com/doi/10.1002/pep.3678)

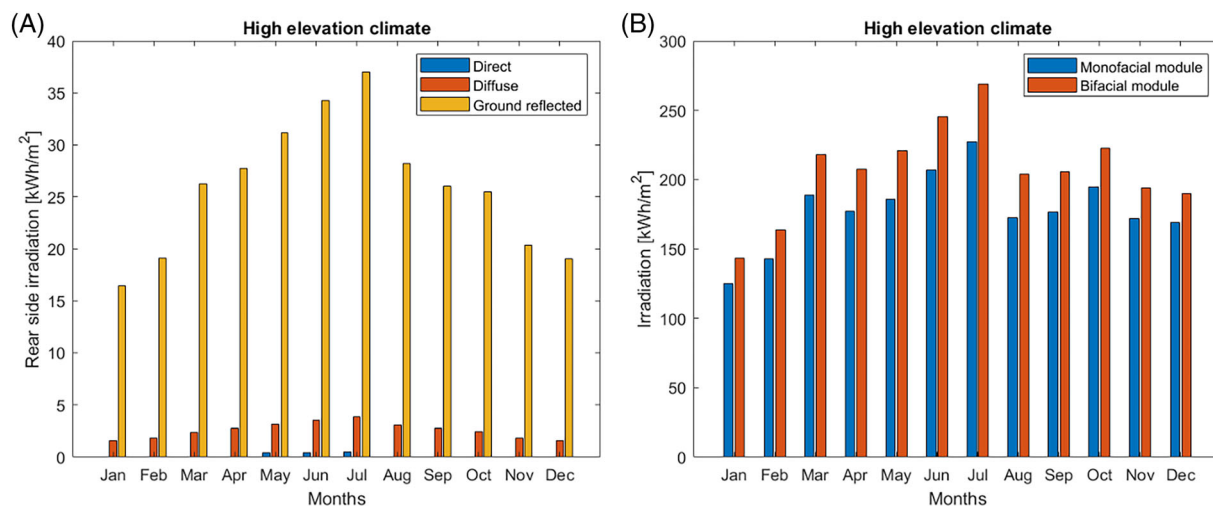


**FIGURE A4** Results of our rear irradiance model applied to the high elevation climate data. (a) Distribution of light on the rear of the PV module. (b) Comparison of monthly irradiation for mono- and bifacial modules. [Colour figure can be viewed at [wileyonlinelibrary.com](https://onlinelibrary.wiley.com/doi/10.1002/pep.3678)] [wileyonlinelibrary.com](https://onlinelibrary.wiley.com/doi/10.1002/pep.3678)

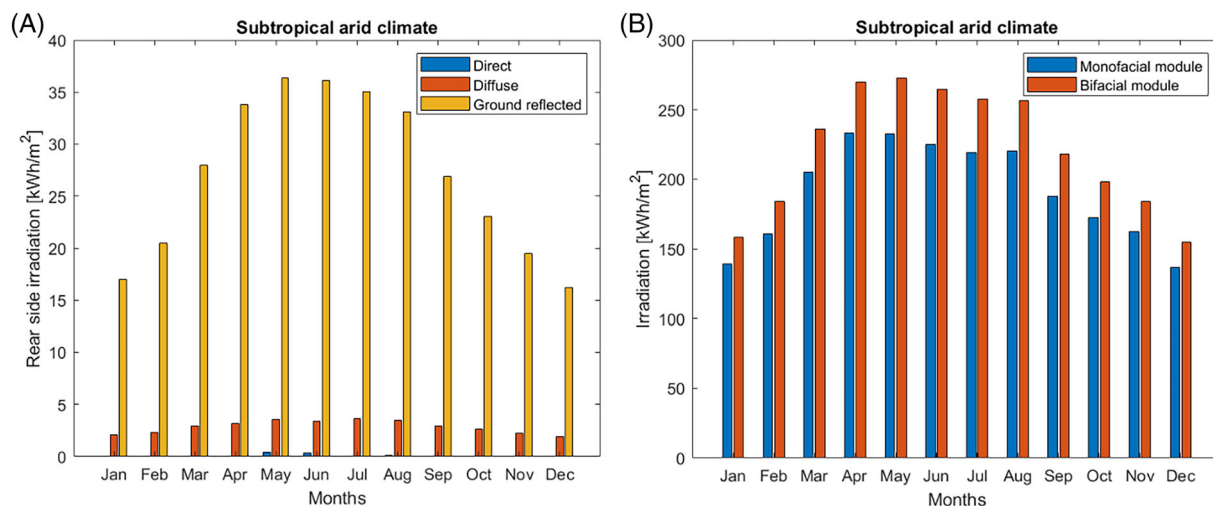


**FIGURE A5** Results of our rear irradiance model applied to the subtropical arid climate data. (a) Distribution of light on the rear of the PV module. (b) Comparison of monthly irradiation for mono- and bifacial modules. [Colour figure can be viewed at [wileyonlinelibrary.com](https://onlinelibrary.wiley.com/doi/10.1002/pep.3678)] [wileyonlinelibrary.com](https://onlinelibrary.wiley.com/doi/10.1002/pep.3678)